DFT Study of the Glutathione Peroxidase-Like Activity of Phenylselenol Incorporating Solvent-Assisted Proton Exchange

Craig A. Bayse*

Department of Chemistry and Biochemistry, Old Dominion University, Hampton Boulevard, Norfolk, Virginia 23529

Received: March 22, 2007; In Final Form: June 1, 2007

Modeling of the glutathione peroxidase-like activity of phenylselenol has been accomplished using density-functional theory and solvent-assisted proton exchange (SAPE). SAPE is a modeling technique intended to mimic solvent participation in proton transfer associated with chemical reaction. Within this method, explicit water molecules incorporated into the gas-phase model allow relay of a proton through the water molecules from the site of protonation in the reactant to that in the product. The activation barriers obtained by SAPE for the three steps of the GPx-like mechanism of PhSeH fall within the limits expected for a catalytic system at physiological temperatures ($\Delta G_1^{\ddagger} = 19.1$ kcal/mol; $\Delta G_2^{\ddagger} = 6.6$ kcal/mol; $G_3^{\ddagger} = 21.7$ kcal/mol) and are significantly lower than studies which require direct proton transfer. The size of the SAPE network is also considered for the model of the reduction of the selenenic acid, step 2 of the GPx-like cycle. Use of a four-water network better accommodates the reaction pathway and reduces the activation barrier by 5 kcal/mol over the two-water model.

Introduction

Selenium is an essential nutrient important for its role in the modulation of oxidative stress.[1] The glutathione peroxidases (GPx) are a family of protective selenoproteins that scavenge reactive oxygen species (ROS), culprits in cellular damage and oxidative stress, factors which increase risk of cancer,[2] cardiovascular disease,[3] and various inflammatory illnesses.[4] In addition to GPx and other antioxidant selenoenzymes, small selenium metabolites have been shown to supplement enzymatic regulation of ROS to reduce risk of disease.[5] Synthetic mimics of GPx[6] have been of interest as potential chemopreventives with lower toxicity than these metabolites. Two GPx mimics (defined here as small selenium compounds that catalytically reduce ROS) are in clinical trials as chemopreventatives against stroke (ebselen)[7] and cancer (selenomethionine).[8] Further development of synthetic organoselenium chemopreventatives would be enhanced by a more complete understanding of the mechanisms by which these compounds scavenge ROS.

Redox catalysis by GPx occurs at the active site selenocysteine (SeCys) residue, an amino acid found in all selenoproteins.[9] In the resting state, SeCys is in the selenol (RSeH) form which is oxidized to selenenic acid (RSeOH) by ROS. This oxidized form is reduced in two steps through a selenenyl sulfide (RSeSR′) intermediate to regenerate the selenol (Scheme 1).[10] Small molecule mimics of this enzyme operate by similar mechanisms.[6b] In this study, we build upon our previous work[11] on small molecule mimics by modeling the solution-phase reactivity of a simple selenol, PhSeH, the catalytic cycle of which is directly analogous to the mechanism shown in Scheme 1. Phenylselenol is the parent of many aryl selenols which are important targets for chemoprevention because, unlike their alkylselenols counterparts, they are generally not metabolized into toxic byproducts.[5]

The challenge to computational modeling of the mechanism in Scheme 1 lies in the role played by the aqueous solvent.

SCHEME 1: Mechanism for Catalytic Scavenging of Reactive Oxygen Species by Selenols

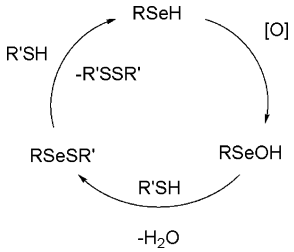

Each of the mechanistic steps involves exchange of a proton from one heavy atom to another, processes that are facilitated by weak acid/base interactions with the surrounding solvent. Incorporating solvent effects by typical means (such as implicit solvation fields[12] and explicit solvation through hydrid quantum mechanical/molecular mechanical (QM/MM)[13] modeling) only account for solvation and do not model direct involvement of solvent molecules in a mechanistic step. Several groups[14] have included explicit molecules of solvation in their gas-phase models to facilitate proton exchange by connecting the sites of protonation with a network of solvent molecules. As the reaction progresses along the reaction pathway, a proton is relayed through the network to the site of protonation in the product. The solvent network is intended to mimic (in a first approximation) the role of solvent in a process involving proton exchange rather than to reproduce solvation of the chemical system. This technique, referred to here as solvent-assisted proton exchange (SAPE) to distinguish it from microsolvation methods that use explicit molecules solely for the purpose of solvation, is related to the proton shuttle mechanism important for many enzymes (i.e., carbonic anhydrase[15]).

In this article, we use SAPE to model the mechanism of the GPx-like catalytic cycle of PhSeH, the mechanistic steps of which are shown in eqs 1−3 and are analogous to those proposed for GPx. Methyl hydrogen peroxide and methylthiol

* To whom correspondence should be addressed.

10.1021/jp072297u CCC: $37.00
Published on Web 08/25/2007

SCHEME 2: SAPE Model for Step 1

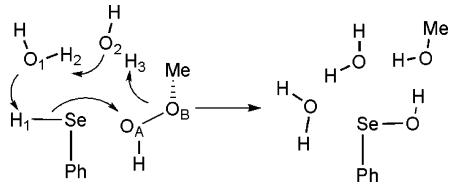

are used as the model oxidizing and reducing agents, respectively.

$$\mathrm{PhSe}\mathit{H} + \mathrm{MeOOH} \rightarrow \mathrm{PhSeOH} + \mathrm{MeO}\mathit{H} \quad (1)$$

$$\mathrm{PhSeOH} + \mathrm{MeS}\mathit{H} \rightarrow \mathrm{PhSeSMe} + \mathit{H}\mathrm{OH} \quad (2)$$

$$\mathrm{PhSeSMe} + \mathrm{MeS}\mathit{H} \rightarrow \mathrm{PhSe}\mathit{H} + \mathrm{MeSSMe} \quad (3)$$

In eqs 1−3, the protons undergoing transfer are italicized in both reactants and products. These protons are not identical between reactant and product because exchange occurs indirectly through the solvent. The reactions 1−3 are mapped from an initial reactant complex that includes the minimum number of water molecules required to bridge the sites of protonation in reactant and product. These initial SAPE complexes were designed separately by (a) assuming the path of reaction in aqueous solution and (b) constructing the solvent network to allow proton exchange for the proposed pathway. Adjustments to the shape and size of the SAPE network can be made to accommodate the assumed reaction pathway. SAPE modeling of the GPx-like cycle of PhSeH presented below successfully provides activation barriers that are realistic for a catalytic process at physiological temperatures. These results are contrasted with previous modeling studies[16,17] of similar GPx-like mechanisms which obtain unrealistically high activation barriers because they do not incorporate some approximation of the direct role of solvent in proton exchange. In comparison, the results below compare favorably with Morokuma's recent DFT study of a model of the active site of GPx which included proton exchange through the protein and explicit water molecules, albeit through different reaction pathways than the present study.[18] Although the goal of this study is not to model the GPx active site, Morokuma's computational results for the enzyme serve as a reference point in the absence of complete experimental data.

Theoretical Methods

Geometry optimizations were performed at the DFT/mPW1PW91[19] level in Gaussian 03.[20] Selenium was represented by the Hurley et al.[21] relativistic effective core potential (RECP) double-ζ basis set augmented with a set of even-tempered s, p, and d diffuse functions. The Wadt-Hay RECP basis set modified with diffuse s and p functions was used for sulfur.[22] Oxygen was represented by Dunning's split-valence triple-ζ plus polarization function basis set (TZVP)[23] augmented with s- and p-type diffuse functions. Carbon basis sets were double-ζ plus polarization quality.[24] Hydrogens attached to non-carbon heavy atoms were TZVP quality, whereas those attached to carbon were double-ζ. Manual conformation searches have been performed to ensure that the reported structures are the lowest mimina within the hydrogen bond connectivity shown in Schemes 2−5 for the reactant complexes. The reported energies include zero-point energy (ZPE), thermal corrections, and bulk solvation effects calculated using the PCM[9] model. The entropy required to form these SAPE complexes in the gas phase has been ignored in the present analysis due to the uncertainty relating this property to solution phase. However, entropy has been included in the reported Gibbs free energies of activation ($\Delta G^{\ddagger}$) which are calculated in reference to the respective reactant complex.

SCHEME 3: Two-Water SAPE Model for Step 2[a]

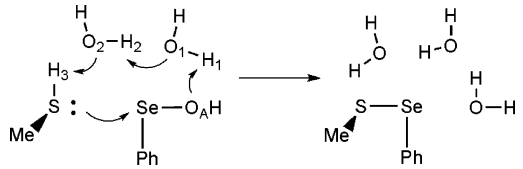

[a] Reaction through an S_N2 process is assumed.

SCHEME 4: Four-Water SAPE Model of Step 2[a]

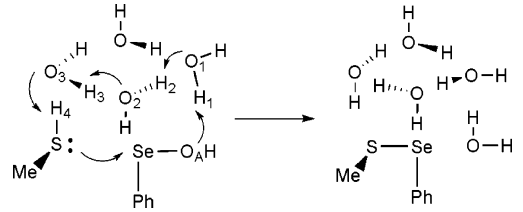

[a] Proton exchange across the water square allows for a more favorable S_N2 process.

SCHEME 5: SAPE Model for Step 3[a]

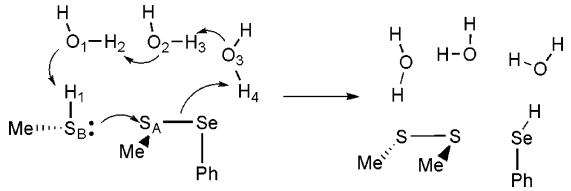

[a] Three water molecules are required to span the heavy atoms for this S_N2 process.

TABLE 1: Evolution of Bond Lengths between Heavy Atoms and within the SAPE Network for Step 1[a]

d, Å	R	TS	P
$Se-O_A$	3.519	2.139	1.782
O_A-O_B	1.432	1.928	2.652
O_1-H_1	2.132	1.592	0.976
O_1-H_2	0.975	1.011	1.762
O_2-H_2	1.823	1.574	0.979
O_2-H_3	0.971	1.022	1.734
O_B-H_3	1.874	1.531	0.980
$Se-H_1$	1.481	1.548	2.461

[a] Atomic labeling follows Scheme 2.

Results and Discussion

In the discussion below, the reported stationary points are labeled by their mechanistic step (e.g., $\mathbf{1_R}$ is the reactant complex for step 1). Selected structural information is reported in Figure 1 and Tables 1−4. The energetics in Table 5 are reported as ΔH and $\Delta G^{\ddagger}$ corrected for solvation effects.

For step one of the GPx-like cycle of PhSeH (eq 1), oxidation of selenium was assumed to proceed by the transfer of OH^+ from MeOOH to the selenol. The bulk solvent neutralizes the basic methoxide and deprotonates the selenol. To mimic this process, a hydrogen-bonding network of two water molecules was placed between the selenol proton and the methoxy oxygen (Scheme 2). Figure 1a shows the optimized structure of the initial complex $\mathbf{1_R}$. From this structure, the transition state for electrophilic attack $\mathbf{1_{TS}}$ was found to have an activation enthalpy of 12.7 ($\Delta G^{\ddagger}$ = 19.1) kcal/mol. The imaginary frequency corresponding to $\mathbf{1_{TS}}$ (Figure 1a) is consistent with the molecular

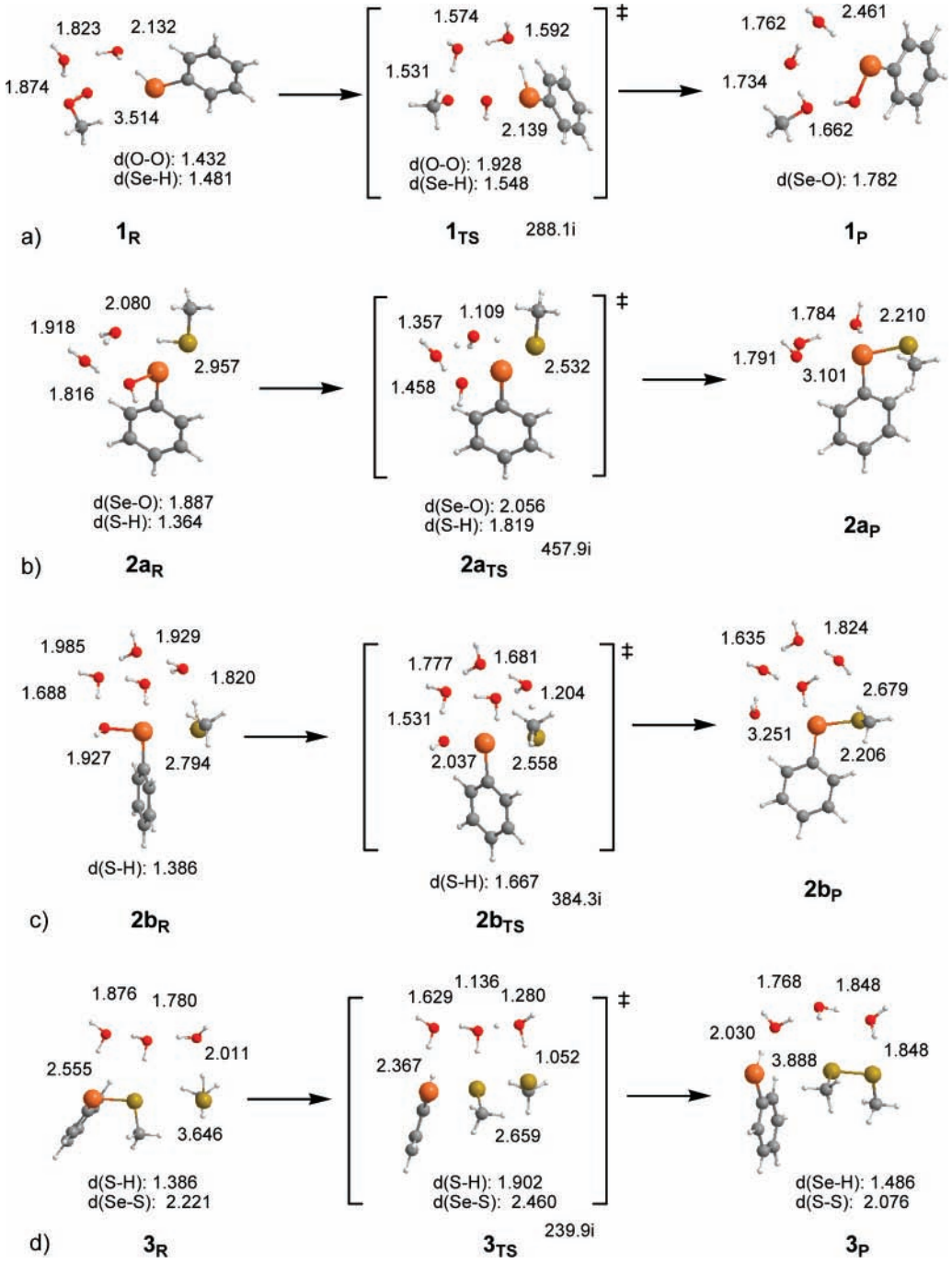

Figure 1. Selected geometric data for the stationary points of the GPx-like mechanism of PhSeH using MeOOH as the oxidant and MeSH as the reductant determined by SAPE models: (a) oxidation of the selenol, (b) reduction of the selenenic acid (two-water SAPE network), (c) reduction of the selenenic acid (four-water SAPE network), and (d) regeneration of the selenol. The stationary points are labeled as reactants (R), transition states (TS), or products (P) for the respective mechanistic steps. Distances are given in angstroms.

motion along the reaction coordinate: the breaking and forming of bonds between the heavy atoms (O−O and Se−O, respectively) concerted with "transfer" of the selenol proton through the SAPE network to the methoxy oxygen. The progression of the bond distances within the SAPE network is listed in Table 1. At $\mathbf{1_{TS}}$, the hydrogen bonds in $\mathbf{1_R}$ have shortened considerably, whereas the O−H bonds lengthen by less than 0.05 Å. Proton transfer through the SAPE network is driven by the increased negative charge on the methoxy oxygen formed as the O−O bond is broken ($\Delta q = -0.185$e). The post-TS structure was fully optimized to $\mathbf{1_P}$ (PhSeOH, shown in Figure 1a) which lies 59.1 kcal/mol below the reactant complex $\mathbf{1_R}$. Note that the selenol proton is now part of the water network.

TABLE 2: Evolution of Bond Lengths between Heavy Atoms and within the Two-Water SAPE Network for Step 2a[a]

d, Å	R	TS	P
Se−O_A	1.877	2.056	3.101
Se−S	2.957	2.532	2.210
S−H_1	1.364	1.819	3.493
O_1−H_1	2.080	1.109	0.973
O_1−H_2	0.974	1.103	1.784
O_2−H_2	1.918	1.357	0.978
O_2−H_3	0.976	1.049	1.791
O_A−H_3	1.816	1.458	0.978

[a] Atomic labeling follows Scheme 3.

TABLE 3: Evolution of Bond Lengths between Heavy Atoms and within the Four-Water SAPE Network for Step 2b[a]

d, Å	R	TS	P
Se−S	2.794	2.558	2.206
Se−O_A	1.927	2.037	3.251
O_A−H_1	1.688	1.531	0.972
O_1−H_1	0.991	1.023	1.882
O_1−H_2	1.985	1.840	1.000
O_2−H_2	0.969	0.979	1.635
O_2−H_3	1.929	1.659	0.985
O_3−H_3	0.973	1.002	1.752
O_3−H_4	1.820	1.204	0.964
S−H_4	1.386	1.667	2.679

[a] Atomic labeling follows Scheme 4.

TABLE 4: Evolution of Bond Lengths between Heavy Atoms and within the SAPE Network for Step 3[a]

d, Å	R	TS	P
Se−S_A	2.221	2.460	3.888
S_A−S_B	3.646	2.659	2.076
S_B−H_1	1.364	1.902	2.426
O_1−H_1	2.011	1.057	0.970
O_1−H_2	0.979	1.280	1.848
O_2−H_2	1.780	1.136	0.974
O_2−H_3	0.973	1.001	1.768
O_3−H_3	1.876	1.629	0.980
O_3−H_4	0.970	0.986	2.030
Se−H_4	2.555	2.367	1.486

[a] Atomic labeling follows Scheme 5.

TABLE 5: Reaction Enthalpies (ΔH)[a] and Activation Gibbs Free Energies ($\Delta G^{\ddagger}$)[b] for the Three Mechanistic Steps of the Catalytic Scavenging of MeOOH by PhSeH[c]

	R	TS	P
1, ΔH^{a}	0.0	12.7	−59.1
$\Delta G^{\ddagger,b}$		19.1, *45−48*,[g] *57.6*,[h] *32.5*,[i] *17.1*[j]	
2a, $\Delta H^{a,d}$	−50.1 (0.0)	−45.2 (4.9)	−76.1 (−26.0)
$\Delta G^{\ddagger,b}$		11.1, *27.1*,[g] *17.9*[j]	
2b, $\Delta H^{a,e}$	−53.0 (0.0)	−50.5 (2.5)	−77.0 (−24.0)
$\Delta G^{\ddagger,b}$		6.6	
3, $\Delta H^{a,f}$	−63.1 (0.0)	−48.3 (14.8)	−56.8 (6.3)
$\Delta G^{\ddagger,b}$		21.7, *57.0*,[g] *21.5*[j]	

[a] Enthalpies are referenced to the SAPE reactant complex 1_R + 2MeSH + $2H_2O$. [b] $\Delta G^{\ddagger}$ values are referenced to the SAPE reactant complex for each individual step. [c] Values have been corrected for zero-point energy and bulk solvation. [d] Includes $2H_2O$ + MeSH + MeOH for mass balance with **1**. [e] Includes MeSH + MeOH for mass balance with 1. [f] Includes $2H_2O$ + MeOH for mass balance with **1**. [g] Reference 16, $\Delta E^{\ddagger}$ + ZPE. [h] Reference 17a, $\Delta G^{\ddagger}$ [i] Reference 17b, $\Delta G^{\ddagger}$. [j] Reference 18, $\Delta H^{\ddagger}$.

The second step (eq 2) was assumed to proceed by an S_N2-type process: backside attack of the thiol on the selenenic acid with water as the leaving group. The thiol can form a stable complex with the selenenic acid by donating electron density into the Se−O antibonding orbital.[25] From this complex, a minimum of two water molecules are required to connect the thiol proton to the selenenic acid oxygen by a hydrogen bond network while maintaining trans coordination of the thiol (Scheme 3). This two-water SAPE model for the reactant complex $\mathbf{2a_R}$ optimizes to an ∠S−Se−O angle (161.7°) smaller than the optimal 180° for an S_N2 attack. At the transition state, the bonds forming between sulfur and selenium are coupled to transfer of a proton through the water network to the leaving OH group. The activation energy for $\mathbf{2a_{TS}}$ is 5.8 ($\Delta G^{\ddagger}$ = 11.1) kcal/mol. As in step 1, the increasing charge on OH allows it to pull a proton from the solvent network, resulting in the deprotonation of the thiol (Scheme 2). The product complex $\mathbf{2a_P}$ (PhSeSMe) is exothermic (−25.2 kcal/mol) and includes a weak donor−acceptor interaction between the leaving water and the selenenyl sulfide.

Several groups have shown that activation barriers for microsolvated reaction complexes can vary depending upon the number of solvent molecules included in the model.[14c,14e,26] This possibility has been tested on the second step of the GPx cycle. A square SAPE network of four water molecules (Scheme 3)[27] was built to allow for transfer of the proton across the square with less strain than the two-water model in **2a**. The resulting ∠S−Se−O angle for the reactant complex $\mathbf{2b_R}$ was closer to ideal (172.4° (Figure 1c)) and allowed the thiol to form a stronger interaction with the selenium (NBO:[28] $\mathbf{2a_R}$: $\Delta E_{d\rightarrow a}$ = 15.5 kcal/mol; $\mathbf{2b_R}$: $\Delta E_{d\rightarrow a}$ = 28.9 kcal/mol). The more favorable geometry for the S_N2 process results in a much lower activation enthalpy (2.5 kcal/mol ($\Delta G^{\ddagger}$ = 6.6)) for $\mathbf{2b_{TS}}$, consistent with the ease with which selenenic acids are reduced by thiols. The products for this model are slightly more exothermic than those for the two-water SAPE model **2a** (−24.0 kcal/mol).

The changes in bond distance over the two- and four-water SAPE models **2a** and **2b** are listed in Tables 2 and 3. A key difference between these pathways is the length of the S−H bond in the transition state. Whereas in $\mathbf{2b_{TS}}$ this bond is extended by 0.28 Å, the S−H bond in $\mathbf{2a_{TS}}$ is broken due to strain and the proton has joined the SAPE network. The greater similarity between the four-water SAPE model and the expectations of an S_N2 process and the lower barrier to activation make the four-water model a better model for this mechanistic step.

The last step of the GPx cycle in which the selenol is regenerated (eq 3) was modeled as an S_N2 attack of the thiol on the S of the selenenyl sulfide (Scheme 4). The longer Se−S distance in this step required three water molecules to span the sites of protonation in the reactant and product complexes. The reactant complex $\mathbf{3_R}$ shown in Figure 1d has a long nonbonded interaction between the two sulfur atoms and a ∠S−S−Se of 172.9°. The changes in the bond distances for this step are listed in Table 4. At $\mathbf{3_{TS}}$, the thiol proton has transferred to the solvent network and couples proton transfer through the water network to the displacement of Se from the selenenyl sulfide by thiol. The structure of the TS is suggestive of the presence of a zwitterionic intermediate, but, analysis of the reaction pathway suggests that it is concerted: no charge-separated intermediate was found. The activation enthalpy for this step (14.8 ($\Delta G^{\ddagger}$ = 21.7) kcal/mol) is the highest along the reaction pathway, consistent with experimental observations of regeneration of the selenol being the rate-determining step. The product complex $\mathbf{3_P}$ is slightly endothermic (Table 1), consistent with H_{rxn} for eq 3.

Exchange reactions bearing structural, but not energetic, similarities to those in steps 2 and 3 of the GPx-like cycle have been shown for the gas-phase substitution of a chalcogenate (for example: eq 4).[26,29] The profile of this reaction shows a stable intermediate rather than an S_N2-type transition state.

$$X^- + RSSR \rightarrow [XSR(SR)]^- \rightarrow RSX + RS^- \qquad (4)$$

A stable intermediate is formed because (a) delocalization of the negative charge over multiple centers is favorable in the gas phase and (b) sulfur and heavier chalcogens are able to expand their octet to form the hypervalent intermediate. Equations 2 and 3 differ from eq 4 because the former require proton exchange to occur in addition to substitution. In eq 4, the negative charge is maintained throughout the process and is a

contributing factor to the existence of the stable intermediate. In eq 2 or 3, an analogous intermediate requires that the proton be transferred to the solvent network either before or after Se−S or S−S bond formation. The resulting charge-separated intermediate would be unfavorable in the gas-phase for a weak base such as water. As a result, substitution is forced to be concerted with proton exchange to minimize charge separation along the reaction pathway. For example, in the mapping of the reaction pathway for step 2 by incremental increase of the S−H bond, deprotonation of the thiol was concomitant with heavy atom bond breaking and forming and no charge-separated intermediate was found for either **2a** or **2b**. In solution phase, bulk water could sufficiently delocalize the proton charge to allow formation of the charge-separated intermediate. Models using larger SAPE models could also obtain charge-separated intermediates. If enough solvent molecules were included in the model, it is possible that the proton charge could be sufficiently delocalized to allow a stable charge-separated intermediate to form. The small size of the networks shown in Schemes 2−5 ensures that the proton exchange will be concerted with heavy-atom bond breaking and forming, because there are too few solvent molecules available to delocalize charge and allow a zwitterionic intermediate. Nonetheless, SAPE modeling allows us to obtain qualitative information about the activation energies otherwise impossible in gas-phase theory. These values are likely upper bounds to the stepwise pathway as the transition state for simple transfer of the proton to the solvent network should be similar to or lower than the concerted pathways.

Proton transfer through the model protein and explicit water molecules was an integral part of Morokuma's recent computational study of the mechanism of GPx, but the specifics of the model lead to stepwise pathways. In the GPx transition state for step 1, oxidation of the selenol occurs by first transferring the selenol proton to the carbonyl oxygen of the nearby Gln followed by oxidation of the selenolate. The GPx model active site allows an initial deprotonation step because (a) the amide carbonyl is more basic than water and (b) the larger model delocalizes the positive charge over a greater number of atoms than is possible in our limited SAPE model. Both Morokuma's stepwise and our concerted barriers are comparable to the experimental barrier of 14.9 kcal/mol[18] and the barrier ($\Delta G^{\ddagger}$ = 16.4 kcal/mol (MP2)) found for the oxidation of methylselenolate by hydrogen peroxide.[30,31] The barriers for step three are also similar between models despite modeling the pathway as stepwise or concerted. However, comparison of the GPx and SAPE models reveal important differences in model design that lead to a 10 kcal/mol difference in $\Delta H^{\ddagger}$ (Table 5) for step 2 of the mechanism. The best PhSeH model assumes an S_N2-type attack using four water molecules to relay the proton. The Gpx model does not assume an S_N2 pathway and adds one water molecule for attack of the thiol at a ~90° angle to the leaving group. However, the sterics of the GPx active site may not allow the proper orientation of the thiol for a backside attack. If so, computational modeling has revealed an important distinction between the enzymatic mechanism and that of the solution-phase mimic.

Conclusions

A mechanism for redox scavenging by PhSeH has been determined using networks of explicit water molecules to mimic the role of solvation. The activation barriers of the computed reaction pathway summarized in Table 5 are consistent with a catalytic process at physiological temperature and similar to those obtained in Morokuma's DFT study of a model of the GPx active site which incorporates proton exchange through the protein backbone and explicit water molecules. Comparison of these results to prior gas-phase computational studies shows that solvent networks are essential to obtain reasonable activation barriers for a catalytic pathway at physiological temperatures. Specifically, the activation energies for the SAPE models are much lower than those for theoretical models[16,17] that do not include a water network (Table 5). The lack of solvent participation requires strained transition states and unusual intermediates unlikely to be found in solution phase (albeit reasonable for a gas-phase process). The associated activation barriers are too high for catalytic activity even after correction for bulk solvation. The approximate solvent environment included by SAPE modeling avoids these unrealistic (for aqueous phase) transition states.

SAPE modeling represents a step forward in modeling of the aqueous phase chemistry of these reactions. Despite the question of the reliability of the SAPE networks for models of bulk solvent, reasonable barriers are obtained for the GPx-like cycle of PhSeH. Further development of the use of SAPE networks will require examination of the size of network required for adequate representation of the weak acid/base catalysis by the solvent. The success of applying SAPE modeling techniques to this and other aqueous-phase problems represents an important step forward in understanding the role of solvent in chemical reactivity.

Acknowledgment. The authors thank the Thomas F. Jeffress and Kate Miller Jeffress Memorial Trust for support of this research.

References and Notes

(1) (a) Ganther, H. E. *Carcinogenesis* **1999**, *20*, 1657. (b) Nordberg, J.; Arner, E. S. J. *Free Rad. Biol. Med.* **2000**, *31*, 1287. (c) *Selenium: Its Molecular Biology and Role in Human Health*; Hatfield, D. L., Berry, M. J., Gladyshev, V. N., Eds.; Springer: New York, 2006. (d) Kayanoki, Y.; Fujii, J.; Islam, K. N.; Suzuki, K.; Kawata, S.; Matsuzawa, Y.; Taniguchi, N. *J. Biochem.* **1996**, *119*, 817.

(2) (a) Wiseman, H.; Halliwell, B. *Biochem. J.* **1996**, *313*, 17. (b) Darleyusmar, V.; Wiseman, H.; Halliwell, B. *FEBS Lett.* **1995**, *369*, 131. (c) Halliwell, B. *Ann. Rev. Nutrit.* **1996**, *16*, 33. (d) Klaunig, J. E.; Kamendulis, L. M. *Ann. Rev. Pharmacol. Toxicol.* **2004**, *44*, 239.

(3) (a) Touyz, R. M.; Schiffrin, E. L. *Histochem. Cell. Biol.* **2004**, *122*, 339. (b) Madamanchi, N. R.; Vendrov, A.; Runge, M. S. *Arterioscler. Thromb. Vasc. Biol.* **2005**, *25*, 29.

(4) (a) Rayman, M. P. *Lancet* **2000**, *356*, 233. (b) Kohrle, J.; Brigelius-Flohé, R.; Bock, A.; Gartner, R.; Meyer, O.; Flohé, L. *Biol. Chem.* **2000**, *381*, 849.

(5) Ganther, H. E.; Lawrence, J. R. *Tetrahedron* **1997**, *53*, 12299.

(6) (a) Mugesh, G.; Singh, H. B. *Chem. Soc. Rev.* **2000**, *29*, 347. (b) Mugesh, G.; du Mont, W.-W.; Sies, H. *Chem. Rev.* **2001**, *101*, 2125.

(7) Lapchak, P. A.; Zivin, J. A. *Stroke* **2003**, *34*, 2013.

(8) Lippman, S. M.; Goodman, P. J.; Klein, E. A.; Parnes, H. L.; Thompson, I. M.; Kristal, A. R.; Santella, R. M.; Probstfield, J. L.; Moinpour, C. M.; Albanes, D.; Taylor, P. R.; Minasian, L. M.; Hoque, A.; Thomas, S. M.; Crowley, J. J.; Gaziano, J. M.; Stanford, J. L.; Cook, E. D.; Fleshner, N. E.; Lieber, M. M.; Walther, P. J.; Khuri, F. R.; Karp, D. D.; Schwartz, G. G.; Ford, L. G.; Coltman, C. A. *J. Natl. Cancer Inst.* **2005**, *97*, 94−102.

(9) (a) Gromer, S.; Eubel, J. K.; Lee, B. L.; Jacob, J. *Cell. Mol. Life Sci.* **2005**, *62*, 2414. (b) Stadtman, T. C. *Ann. Rev. Biochem.* **1990**, *59*, 111. (c) Birringer, M.; Pilawa, S.; Flohé, L. *Nat. Prod. Rep.* **2002**, *19*, 693. (d) Flohé, L. *Curr. Top. Cell. Regul.* **1985**, *27*, 473.

(10) Epp, O.; Ladenstein, R.; Wendel, A. *Eur. J. Biochem.* **1983**, *133*, 51.

(11) (a) Bayse, C. A.; Allison, B. D. *J. Mol. Model.* **2007**, *13*, 47. (b) Ritchey, J. A.; Davis, B. M.; Pleban, P. A.; Bayse, C. A. *Org. Biomol. Chem.* **2005**, *3*, 4337.

(12) Tomasi, J.; Mennuci, B.; Cammi, R. *Chem. Rev.* **2005**, *105*, 2999.

(13) (a) Woo, T. K.; Cavallo, L.; Ziegler, T. *Theor. Chem. Acc.* **1998**, *100*, 307. (b) Rega, N.; Iyengar, S.S.; Voth, G.A.; Schlegel, H.B. Vreven, T.; Frisch, M. J. *J. Phys. Chem. B* **2004**, *108*, 4210.

(14) For example: (a) Gorb, L.; Asensio, A.; Tunon, I.; Ruiz-Lopez, M. F. *Chem. Eur. J.* **2005**, *11*, 6743. (b) Mujika, J. I.; Mercero, J. M.;

Lopez, X. *J. Am. Chem. Soc.* **2005**, *127*, 4445. (c) Wu, Z. J.; Ban, F. Q.; Boyd, R. J. *J. Am. Chem. Soc.* **2003**, *125*, 6994. (d) Kallies, B.; Mitzner, R. *J. Mol. Model*. **1998**, *4*, 183. (e) Akdag, A.; McKee, M. L.; Worley, S. D. *J. Phys. Chem. A* **2006**, *110*, 7621.

(15) Lindskog, S. *Pharmacol. Therap.* **1997**, *74*, 1.

(16) Benkova, Z.; Kóňa, J.; Gann, G.; Fabian, W. M. F. *Int. J. Quant. Chem.* **2002**, *90*, 555.

(17) (a) Pearson, J. K.; Boyd, R. J. *J. Phys. Chem. A* **2006**, *110*, 8979. (b) Pearson, J. K.; Boyd, R. J. *J. Phys. Chem. A* **2007**, *111*, 3152.

(18) Prabhakar, R.; Vreven, T.; Morokuma, K.; Musaev, D. G. *Biochemistry* **2005**, *44*, 11864.

(19) Adamo, C.; Barone, V. *J. Chem. Phys.* **1998**, *108*, 664.

(20) Frisch, M. J.; Trucks, G. W.; Schlegel, H. B.; Scuseria, G. E.; Robb, M. A.; Cheeseman, J. R.; Montgomery, J. A., Jr.; Vreven, T.; Kudin, K. N.; Burant, J. C.; Millam, J. M.; Iyengar, S. S.; Tomasi, J.; Barone, V.; Mennucci, B.; Cossi, M.; Scalmani, G.; Rega, N.; Petersson, G. A.; Nakatsuji, H.; Hada, M.; Ehara, M.; Toyota, K.; Fukuda, R.; Hasegawa, J.; Ishida, M.; Nakajima, T.; Honda, Y.; Kitao, O.; Nakai, H.; Klene, M.; Li, X.; Knox, J. E.; Hratchian, H. P.; Cross, J. B.; Bakken, V.; Adamo, C.; Jaramillo, J.; Gomperts, R.; Stratmann, R. E.; Yazyev, O.; Austin, A. J.; Cammi, R.; Pomelli, C.; Ochterski, J. W.; Ayala, P. Y.; Morokuma, K.; Voth, G. A.; Salvador, P.; Dannenberg, J. J.; Zakrzewski, V. G.; Dapprich, S.; Daniels, A. D.; Strain, M. C.; Farkas, O.; Malick, D. K.; Rabuck, A. D.; Raghavachari, K.; Foresman, J. B.; Ortiz, J. V.; Cui, Q.; Baboul, A. G.; Clifford, S.; Cioslowski, J.; Stefanov, B. B.; Liu, G.; Liashenko, A.; Piskorz, P.; Komaromi, I.; Martin, R. L.; Fox, D. J.; Keith, T.; Al-Laham, M. A.; Peng, C. Y.; Nanayakkara, A.; Challacombe, M.; Gill, P. M. W.; Johnson, B.; Chen, W.; Wong, M. W.; Gonzalez, C.; Pople, J. A. *Gaussian 03*, revision C.02; Gaussian, Inc.: Wallingford, CT, 2004.

(21) Hurley, M. M.; Pacios, L. F.; Christiansen, P. A.; Ross, R. B.; Ermler, W. C. *J. Chem. Phys.* **1986**, *84*, 6840.

(22) Wadt, W. R.; Hay, P. J. *J. Chem. Phys.* **1985**, *82*, 284.

(23) Dunning, T. H. *J. Chem. Phys.* **1971**, *55*, 716.

(24) Dunning, T. H. *J. Chem. Phys.* **1970**, *53*, 2823.

(25) Bayse, C. A.; Baker, R. A.; Ortwine, K. N. *Inorg. Chim. Acta* **2005**, *358*, 3849 and references therein.

(26) Hayes, J. M.; Bachrach, S. M. *J. Phys. Chem. A* **2003**, *107*, 7952.

(27) Note that the water networks obtained by our SAPE models of step 2 resemble those of ref 21 where the solvent molecules are used to explicitly solvate the system (no proton exchange occurs).

(28) Reed, A. E.; Curtiss, L. A.; Weinhold, F. *Chem. Rev.* **1988**, *88*, 899.

(29) Bachrach, S. M.; Pereverzev, A. *Org. Biomol. Chem.* **2005**, *3*, 2095 and references therein.

(30) Cardey, B.; Enescu, M. *Chem. Phys. Chem.* **2005**, *6*, 1175.

(31) The reaction pathway modeled by Cardey and Enescu includes a post-transition state proton exchange where the initially formed MeSeOH and OH^- rearrange to $MeSeO^-$ and H_2O. This proton exchange is independent of the oxidation of the selenolate.